RNF125-mediated ubiquitination of MCM6 regulates the proliferation of human liver hepatocellular carcinoma cells

XUEYI FENG[1,2*], DONGQIANG SONG[3*], XIAOLAN LIU[4*], YONGKANG LIANG[1,2*], PIN JIANG[2], SHENWEI WU[2] and FUBAO LIU[1]

[1]Department of General Surgery, The First Affiliated Hospital of Anhui Medical University, Hefei, Anhui 230022; [2]Department of General Surgery, Lu'an Affiliated Hospital of Anhui Medical University, Lu'an, Anhui 237005; [3]Liver Cancer Institute, Zhongshan Hospital of Fudan University, Shanghai 200032; [4]Department of Gastroenterology, The Affiliated Hospital of Qingdao University, Qingdao, Shandong 266003, P.R. China

Received August 24, 2023; Accepted December 20, 2023

DOI: 10.3892/ol.2024.14238

Abstract. Hepatocellular carcinoma (HCC) is the third leading cause of cancer-associated mortality worldwide. Minichromosome maintenance proteins (MCMs), particularly MCM2-7, are upregulated in various cancers, including HCC. The aim of the present study was to investigate the role of MCM2-7 in human liver HCC (LIHC) and the regulation of the protein homeostasis of MCM6 by a specific E3 ligase. Bioinformatics analyses demonstrated that MCM2-7 were highly expressed in LIHC compared with corresponding normal tissues at the mRNA and protein levels, and patients with LIHC and high mRNA expression levels of MCM2, MCM3, MCM6 and MCM7 had poor overall survival rates. Cell Counting Kit-8 and colony formation assays revealed that the knockdown of MCM2, MCM3, MCM6 or MCM7 in Huh7 and Hep3B HCC cells inhibited cell proliferation and colony formation. In addition, pull-down, co-immunoprecipitation and ubiquitination assays demonstrated that RNF125 interacts with MCM6 and mediates its ubiquitination. Furthermore, co-transfection experiments indicated that RNF125 promoted the proliferation of HCC cells mainly through MCM6. In summary, the present study suggests that the RNF125-MCM6 axis plays an important role in the regulation of HCC cell proliferation and is a promising therapeutic target for the treatment of LIHC.

Correspondence to: Dr Shenwei Wu, Department of General Surgery, Lu'an Affiliated Hospital of Anhui Medical University, 21 Wanxi West Road, Lu'an, Anhui 237005, P.R. China
E-mail: 13605645189@163.com

Professor Fubao Liu, Department of General Surgery, The First Affiliated Hospital of Anhui Medical University, 218 Jixi Road, Hefei, Anhui 230022, P.R. China
E-mail: liufubao@ahmu.edu.cn

*Contributed equally

Key words: hepatocellular carcinoma, MCM6, proliferation, RNF125, ubiquitination

Introduction

Hepatocellular carcinoma (HCC) is the third most frequent cause of cancer-associated death worldwide and represents a major global health challenge (1,2). Currently, the global five-year survival rate of metastatic HCC is <20% (3). Great progress has been made in the diagnosis and treatment of HCC, but the mortality rate remains unsatisfactory (3,4). According to the stage of the tumor and the condition of the patient, there are various treatment options for HCC. A number of curative treatment options exist for early-stage HCC, including surgical resection, radiofrequency ablation and liver transplantation. However, 80% of patients have unresectable HCC and can only be treated with locoregional therapies such as radiotherapy, transarterial chemoembolization or transarterial radioembolization (2). Due to high relapse rates and drug resistance, the prognosis for most HCC patients is less than ideal (5,6). It is therefore imperative to explore new therapeutic targets.

Dysregulated DNA replication in cells is a major contributor to tumor initiation and progression. Minichromosome maintenance proteins (MCMs) are essential for DNA replication and are the subject of considerable research interest (7). The aberrant expression of MCMs has been detected in numerous malignancies, which can lead to genomic instability and uncontrolled cell cycle progression (7,8). The MCM2-7 family is a class of nuclear proteins that contain a highly conserved nucleoside triphosphate binding motif, and are evolutionarily and functionally conserved in eukaryotes (9). Members of the MCM2-7 family have been reported to be upregulated in various cancer tissues and cancer cell lines, including brain tumors, lymphomas, and breast, lung and prostate cancers (10-14). For example, MCM2 has been shown to be associated with the malignant status of lung squamous cell carcinoma and to regulate the proliferation and cell cycle in this type of cancer (13).

MCM6 is an important component of the MCM2-7 complex and is upregulated in a number of tumors, including HCC (15-17). MCM6 promotes the metastasis of HCC via the

MEK/ERK pathway and may serve as a serum biomarker for early recurrence (15). In addition, MCM6 expression is inversely correlated with methyl(R217) human antigen R and is a prognostic marker in non-small cell lung carcinoma (16).

In the present study the role of MCM2-7 in HCC was investigated and the effect of the knockdown of members of this family on the proliferation of human HCC cells was evaluated. The homeostasis of MCM2, MCM3, MCM6 and MCM7 was then investigated. Also, as only MCM6 was found to be mainly degraded by the proteasome pathway, it was selected for further study. Ring finger protein 125 (RNF125) was identified as an E3 ubiquitin ligase for MCM6 and the relationship of these two proteins in HCC was investigated.

Materials and methods

Data analysis using public databases

Gene expression profiling interactive analysis 2 (GEPIA2). GEPIA2 (http://gepia2.cancer-pku.cn) is a tool for the gene expression analysis of sequencing data from The Cancer Genome Atlas and the Tissue Genotype Expression database (18). In the present study, GEPIA2 was used to evaluate the mRNA expression of MCM2-7 and RNF125 in human liver HCC (LIHC) and calculate P-values using Student's t-test; an absolute log2 fold change ≥0.5 and P<0.05 were considered to indicate a significant difference. GEPIA2 was also used to perform a prognostic value analysis by the calculation of overall survival and disease-free survival rates and survival graphs were directly generated by GEPIA2, with the log-rank test the only option for analysis. The associations between different MCMs and the clinical outcomes of LIHC, and the associations between the mRNA expression of certain MCMs and the pathological stage of LIHC were also assessed using GEPIA2.

University of alabama cancer database (UALCAN). UALCAN (http://ualcan.path.uab.edu) is a comprehensive and interactive web resource for the analysis of cancer omics data (19). The protein levels of MCM2-7 in human LIHC were assessed using UALCAN, and Student's t-test was used to generate P-values.

Plasmid construction. Plasmids containing RNF125 and MCM2-7 were purchased from Shanghai Cell Researcher Biotech Co., Ltd. and inserted into empty vectors, which were purchased from Cell Researcher Biotech Co., Ltd.), such as pCDH, pCDNA3.0-Myc, pET22b or pGEX4T-1. Briefly, pCDH-MCM2/MCM3/MCM6/MCM7/RNF125, pCDNA3.0-RNF126-Myc, pET22b-MCM2/MCM3/MCM6/MCM7/RNF125/UBA1/UBCH5A/catalytic core of human ubiquitin specific peptidase 2 (Usp2cc) and pGEX4T-1-MCM6/RNF125 were generated. Mutations were generated in plasmids containing RNF125 or MCM6 by site-directed mutagenesis as previously described (20). Short hairpin RNAs (shRNAs) inserted into the Plko.1 vector targeting RNF125 and MCM2, MCM3, MCM6 and MCM7 were also purchased from Shanghai Cell Researcher Biotech Co., Ltd., and the specific sequences of these shRNAs are shown in Table I.

Cell culture, transfection and reagents. The human HCC cell lines Huh7 and Hep3B were purchased from The Cell Bank of Type Culture Collection of The Chinese Academy of Sciences. These cells were cultured in DMEM (high glucose) supplemented with 10% fetal bovine serum (Gibco; Thermo Fisher Scientific, Inc.) and 100 μg/l penicillin/streptomycin (Gibco; Thermo Fisher Scientific, Inc.). The plasmids were transfected into the cells using Lipofectamine® 2000 (Thermo Fisher Scientific, Inc.), according to the manufacturer's instructions. The ratio of the mass of nucleic acid (plasmid) to the volume of Lipofectamine 2000 was 1:2 (2 μg:4 μl), which was mixed together at room temperature for 20 min, and then added to cells for continued culture at 37˚C. Stably expressed cell lines were generated using puromycin selection (2 μg/ml; Beyotime Institute of Biotechnology) for ≥7 days after 48 h transfection. Cycloheximide (CHX; Selleck Chemicals) was dissolved in dimethyl sulfoxide (Sigma-Aldrich; Merck KGaA) at a concentration of 100 mM and stored at -40˚C. Huh7 and Hep3B cells were treated with 100 μM CHX for 6 h, or at different time periods, at 37˚C. For protein degradation pathway analysis, Huh7 cells were treated with 1 μM proteasomal inhibitor bortezomib (BTZ; Selleck Chemicals) or 20 nM autophagy inhibitor bafilomycin (BAF; Selleck Chemicals) for 6 h at 37˚C prior to western blotting.

Cell proliferation assay. Huh7 and Hep3B cells stably expressing plasmids containing pCDH-MCMs, pCDH-RNF125 or pLKO.1-shMCMs, were seeded in 96-well plates at 5,000 cells/well. These cells were then incubated with Cell Counting Kit-8 (CCK-8) solution (Beyotime Institute of Biotechnology) for 4 h at different time points (0, 24, 48 or 72 h). The 0 h time point was 6 h after the cells were seeded in the plates. The product was then quantified by spectrophotometry at a wavelength of 450 nm using a microplate reader (Bio-Rad Laboratories, Inc.). These experiments were performed with six replicates and repeated three times.

Colony formation assay. Cells stably expressing plasmids containing pCDH-MCMs, pCDH-RNF125 or pLKO.1-shMCMs were seeded into 6-well plates (1,000 cells/well). After 7 days culturing at 37˚C, the cells were fixed with 4% paraformaldehyde (Merck KGaA) for 10 min at room temperature and then stained with 0.2% crystal violet (Beyotime Institute of Biotechnology) at room temperature for 15 min. Images were captured using an iPhone 11 camera (Apple, Inc.) and the number of colonies (≥50 cells) was manually counted using a light-field microscope (CKX53; Olympus, Inc.).

Yeast two-hybrid screening. The yeast two-hybrid (Y2H) screen was performed as described previously (21). Briefly, human MCM6 was used as bait, and its potential E3 ligase was screened from a library containing ~400 open reading frames (ORFs) of human E3 ubiquitin ligases. The positive colony was able to survive in SD-4 medium (deficient in uracil, histidine, leucine and tryptophan) and could be stained with X-Gal (Sangon Biotech Co., Ltd.).

Recombinant protein purification. Hexahistidine (His6)- and glutathione S-transferase (GST)-tagged proteins were purified from the BL21 *E. coli* system as described previously (22). Briefly, after induction with isopropyl-β-d-mercapto-galactopyranoside (Sigma-Aldrich), the cells transfected with

Table I. Sequences of the shRNAs targeting MCM2-7 and RNF125.

shRNA	Target site sequence (5'-3')
shNC	GCGCGATAGCGCTAATAATTT
shMCM2-1	GCACAAGGTACGTGGTGATAT
shMCM2-2	CTATCAGAACTACCAGCGTAT
shMCM2-3	CGCATCCATCTGCGGGACTAT
shMCM2-4	CGAGGAGTGTGTCTCATTGAT
shMCM3-1	GCCTCCATTGATGCTACCTAT
shMCM3-2	GCCACAGATGATCCCAACTTT
shMCM3-3	CCAGGGAATTTATCAGAGCAA
shMCM3-4	CGGCAGGTATGACCAGTATAA
shMCM6-1	CCCGCAGTTTAGAAGTAATTT
shMCM6-2	CCTAACTACTTGCTCGAAGAT
shMCM6-3	CCTTTCTTATAGGCTGGTCTT
shMCM6-4	CCCGATTCGATCTCTTCTTTA
shMCM7-1	GCGCAGATTTGAGCTGTATTT
shMCM7-2	GCTAGTAAGGATGCCACCTAT
shMCM7-3	GTGGACTCAATTTGTGAGAAT
shMCM7-4	GTGGAGAAAGAAGATGTGAAT
shRNF125-1	CCGTTTAATACCCGATGAGAA
shRNF125-2	GAATCACTCGAACACCACATA
shRNF125-3	GCTTGCTGGATCATTGTATTA
shRNF125-4	CTGTCCACTTTGCCGTTTAAT

sh, short hairpin; MCM, minichromosome maintenance protein; RNF125, ring finger protein 125; NC, negative control.

protein-encoding plasmids were centrifuged, lysed in PBS buffer (137 mM NaCl, 2.7 mM KCl, 8 mM Na_2HPO_4 and 2 mM KH_2PO_4, pH 7.4), incubated with Ni^{2+} or glutathione affinity gels, and eluted with 500 mM imidazole or 25 mM reduced L-glutathione solution (pH 8.0). The eluate was then dialyzed in PBS buffer containing 10% glycerol for 6 h at 4˚C and stored at -70˚C.

GST pull-down assay. Purified GST-tagged protein (10 μg), His6-tagged protein (10 μg) and 25 μl Glutathione Sepharose 4B (Sangon Biotech Co., Ltd.) were incubated for 4 h at 4˚C in 800 μl GST pull-down buffer [20 mM Tris-Cl, 5 mM $MgCl_2$, 100 mM NaCl, 1 mM EDTA, 1% NP-40 and fresh 1 mM dithiothreitol (DTT), pH 7.6] supplemented with fresh 10 mg/ml BSA. The samples were pelleted via centrifugation at 500 x g for 3 min at 4˚C and washed five times with GST pull-down buffer. The immunoprecipitates were then denatured in 50 μl of 2X SDS protein loading buffer at 100˚C for 10 min before immunoblotting (IB).

In vitro ubiquitination assay. *In vitro* ubiquitination was performed as described previously (23). Briefly, 50 ng recombinant His6-UBA1 (an E1 or ubiquitin-activating enzyme), 100 ng His6-UBCH5A (an E2 or ubiquitin-conjugating enzyme), 200 ng GST-RNF125 (E3), 200 ng MCM6-His6 and 50 ng His6-ubiquitin were added to *in vitro* ubiquitination buffer (25 mM Tris-Cl, 100 mM NaCl, 5 mM $MgCl_2$, pH 7.8, supplemented with 1 mM fresh ATP and 0.5 mM DTT) to a final volume of 50 μl, and incubated at 37˚C for 1.5 h. Subsequently, 50 ng His6-tagged Usp2cc was added to the tube containing E1, E2, E3 and MCM6 and incubated at 37˚C for a further 30 min. The level of MCM6 ubiquitination was detected by IB analysis using anti-MCM6 antibody.

Co-immunoprecipitation (Co-IP), immunoprecipitation (IP) and IB. For the Co-IP assay, transfected Huh7 and Hep3B cells were lysed in 800 μl Co-IP buffer (50 mM Tris-HCl, 1% NP-40, 150 mM NaCl and 5 mM EDTA, pH 7.6) supplemented with fresh protease inhibitor cocktail (Roche Diagnostics). The cell lysates were then incubated with anti-MCM6 antibody (1:100 dilution; 13347-2-AP; Wuhan Sanying Biotechnology) and 25 μl Protein G magnetic beads (L-1002; Biolinkedin) overnight at 4˚C. For the IP assay, Huh7 and Hep3B cells were lysed in 800 μl RIPA buffer (50 mM Tris-HCl, 150 mM NaCl, 5 mM EDTA, 1% NP-40 and 0.1% SDS, pH 7.6) containing fresh protease inhibitor cocktail. Then, the cell lysates were incubated with the anti-MCM6 antibody (1:100 dilution) and 25 μl Protein G magnetic beads overnight at 4˚C. The next day, the immunoprecipitates were pelleted via centrifugation at 500 x g for 3 min at 4˚C and washed five times with Co-IP/IP buffer. Then, the immunoprecipitates were denaturated for 15 min at 100˚C in 50 μl 2X SDS protein loading buffer. The immunoprecipitates, inputs and other lysates (10 μl) were subjected to 10% SDS-PAGE and transferred to polyvinylidene fluoride membranes (MilliporeSigma). The membranes were blocked with 10% non-fat milk at room temperature for 45 min before incubation with the following antibodies: Anti-MCM2 (1:1,000 dilution; 10513-1-AP), anti-MCM3 (1:1,000 dilution; 15597-1-AP), anti-MCM6 (1:1,000 dilution), anti-MCM7 (1:1,000 dilution; 11225-1-AP), anti-GAPDH (1:6,000 dilution; 60004-1-Ig), anti-RNF125 (1:2,000 dilution; 13290-1-AP), anti-His (1:2,000 dilution; 66005-1-Ig), anti-GST (1:10,000 dilution; HRP-66001) or anti-ubiquitin (1:2,000, 10201-2-AP), all from Wuhan Sanying. The membranes were incubated with primary antibodies overnight at 4˚C, and washed three times with TBST (50 mM Tris-HCl, 150 mM NaCl and 0.2% Tween-20; pH 8.0). Subsequently the membranes were incubated with the following horseradish peroxidase-labeled secondary antibodies: Goat anti-mouse IgG (1:10,000 dilution; SA00001-1) or goat anti-rabbit IgG (1:10,000 dilution; SA00001-2), both from Wuhan Sanying, at room temperature for 2 h and washed three times with TBST. The signals were visualized using high-signal ECL western blotting substrate (cat. no. 180-5001; Tanon Science and Technology Co., Ltd.) and a Tanon 5200 imaging system (Tanon Science and Technology Co., Ltd.).

Statistical analysis. Data are expressed as the mean ± SD and were analyzed by Student's t-test or one-way ANOVA with Tukey's post hoc test using GraphPad Prism 5 (GraphPad Software; Dotmatics). $P<0.05$ was considered to indicate a statistically significant difference.

Results

High expression levels of MCM2-7 in patients with LIHC predict poor overall survival rates. The mRNA and protein expression levels of genes encoding the MCM2-7 complex in

human LIHC were analyzed using the GEPIA2 and UALCAN databases, respectively, and found to be significantly upregulated in LIHC compared with the corresponding normal tissues at the mRNA and protein levels (Fig. 1A and B).

The associations between different MCMs and the clinical outcomes of LIHC were analyzed using GEPIA2 (Fig. 1C). Stronger associations were observed for MCM2, MCM3, MCM6 and MCM7 than for MCM4 and 5. The associations between the mRNA expression of certain MCMs and the pathological stage of LIHC were also assessed using GEPIA2. The mRNA expression levels in the MCM2, MCM3, MCM6 and MCM7 groups were highly variable, and gradually increased with the progression of LIHC in the first three stages, but then markedly decreased in stage IV (Fig. S1A). In addition, patients with LIHC who had high mRNA expression levels of MCM2, MCM3, MCM6 and MCM7 showed poor overall and disease-free survival rates (Figs. 1D and S1B). Therefore, these four genes were selected for further study.

Knockdown of MCMs inhibits the proliferation of HCC cells. shRNAs targeting MCM2, MCM3, MCM6 and MCM7 were constructed and stably transfected into human Huh7 and Hep3B cells. The knockdown efficiencies were detected by IB analysis (Fig. 2A). On the basis of these results, shMCM2-1 and shMCM2-4 for MCM2, shMCM3-2 and shMCM3-4 for MCM3, shMCM6-1 and shMCM6-2 for MCM6, and shMCM7-1 and shMCM7-2 for MCM7 were selected for further study. The viability of Huh7 and Hep3B cells was determined by CCK-8 assay at different time points (0, 24, 48 and 72 h), and cell growth inhibition was observed in the MCM2/3/6/7-knockdown cells compared with that of the negative control (scramble) groups (Fig. 2B). Colony formation assays were also performed, the results of which were highly consistent with those of the CCK-8 assay (Fig. 2C). In addition, wound healing assays were performed and MCM2/3/6/7-knockdown exhibited no evident effect on the migration of Huh7 cells (data not shown).

MCMs promote the proliferation of HCC cells. Huh7 and Hep3B cells were stably transfected with pCDH or pCDH-MCM2/3/6/7 and the expression of the MDMs was detected by IB analysis (Fig. 3A). The viability of the transfected Huh7 and Hep3B cells was then determined by CCK-8 assay at various time points, and cell growth promotion was observed in the pCDH-MCM groups compared with the pCDH control groups (Fig. 3B). The results of colony formation assays were consistent with the results of the CCK-8 assay (Fig. 3C).

RNF125 interacts with MCM6. The pathways of MCM2, MCM3, MCM6 and MCM7 protein degradation were explored. Huh7 cells were treated with the proteasomal inhibitor BTZ or the autophagy inhibitor BAF for 6 h before being subjected to IB analysis. The results shown in Fig. 4A indicate that endogenous MCM6 protein is degraded mainly by the proteasome pathway, and that neither of these degradation pathways affect the other three MCMs. To investigate the regulation of MCM6 protein homeostasis, MCM6 was used as a bait to screen for its interacting partners using the Y2H prey library which contains ~400 ORFs of human E3 ubiquitin ligases. The E3 ligase RNF125 was identified as an interacting partner for MCM6 and verified in yeast cells (Fig. 4B). A direct interaction between RNF125 and MCM6 was detected by GST pull-down assay (Fig. 4C), whereas no interaction of RNF125 with MCM2, MCM3 or MCM7 was found (Fig. 4D). Protein-protein interaction domain analysis revealed that the MCM domain of MCM6 directly interacted with the N-terminal region (1-135 amino acids) of RNF125 containing the RING domain (Fig. 4E). Further Co-IP assays showed that endogenous MCM6 formed a complex with RNF125 in both Huh7 and Hep3B cells (Fig. 4F). These data indicate that RNF125 does indeed interact with MCM6.

RNF125 promotes the ubiquitination and degradation of MCM6. To investigate whether RNF125 affects the stability of the MCM6 protein, Huh7 and Hep3B cells were transfected to express different amounts of RNF125, and the protein levels of MCM6 were detected by IB analysis. The results shown in Fig. 5A show that RNF125 reduced the protein levels of MCM6 in a dose-dependent manner. An *in vitro* ubiquitination assay was carried out, as shown in Fig. 5B. In the presence of E1 (UBA1), E2 (UBCH5A) and E3 (RNF125), the ubiquitination of MCM6 was detectable by IB analysis, and this modification was efficiently attenuated by Usp2cc. Huh7 and Hep3B cells were stably transfected with empty vector (pCDH) or pCDH-RNF125 and the upregulation of RNF125 by pCDH-RNF125 was confirmed by IB analysis (Fig. 5C). The lysates of the transfected Huh7 and Hep3B cells were immunoprecipitated with anti-MCM6 antibody, and the results revealed that the ubiquitination of MCM6 was markedly increased in cells stably expressing pCDH-RNF125 compared with the control cells (Fig. 5D). Three shRNAs targeting RNF125 were designed and tested in human Huh7 and Hep3B cells. shRNF125-2 and shRNF125-3 performed well in the knockdown of RNF125 and were selected for further study (Fig. 5E). The protein levels of endogenous MCM6 were increased in the RNF125-knockdown cells compared with the control cells in the presence of the protein synthesis inhibitor CHX (Fig. 5F). In addition, RNF125 knockdown reduced the ubiquitination of MCM6 and concurrently increased MCM6 protein levels in Huh7 and Hep3B cells (Fig. 5G). These data suggest that RNF125 is an E3 ligase for MCM6 and promotes its degradation.

RNF125 promotes the proliferation of HCC cells mainly through MCM6. pCDH-RNF125 or empty vector (pCDH) was stably transfected into Huh7 and Hep3B cells that also stably expressed scramble shRNA, shMCM6-1 or shMCM6-2, and the protein levels of RNF125 and MCM6 were detected by IB analysis (Fig. 6A). The results of CCK-8 and colony formation assays performed using these cells revealed that RNF125 inhibited the proliferation and colony formation of Huh7 and Hep3B cells with intact MCM6, but not of MCM6 knockdown cells (Fig. 6B and C). These data suggest that RNF125 promotes the proliferation of HCC cells mainly through MCM6. The expression of RNF125 in human LIHC was analyzed using the GEPIA2 database. As shown in Fig. 6D, the expression of RNF125 was downregulated in LIHC compared with normal tissues at the mRNA level. The association between RNF125 and the clinical outcome of LIHC was also analyzed, and

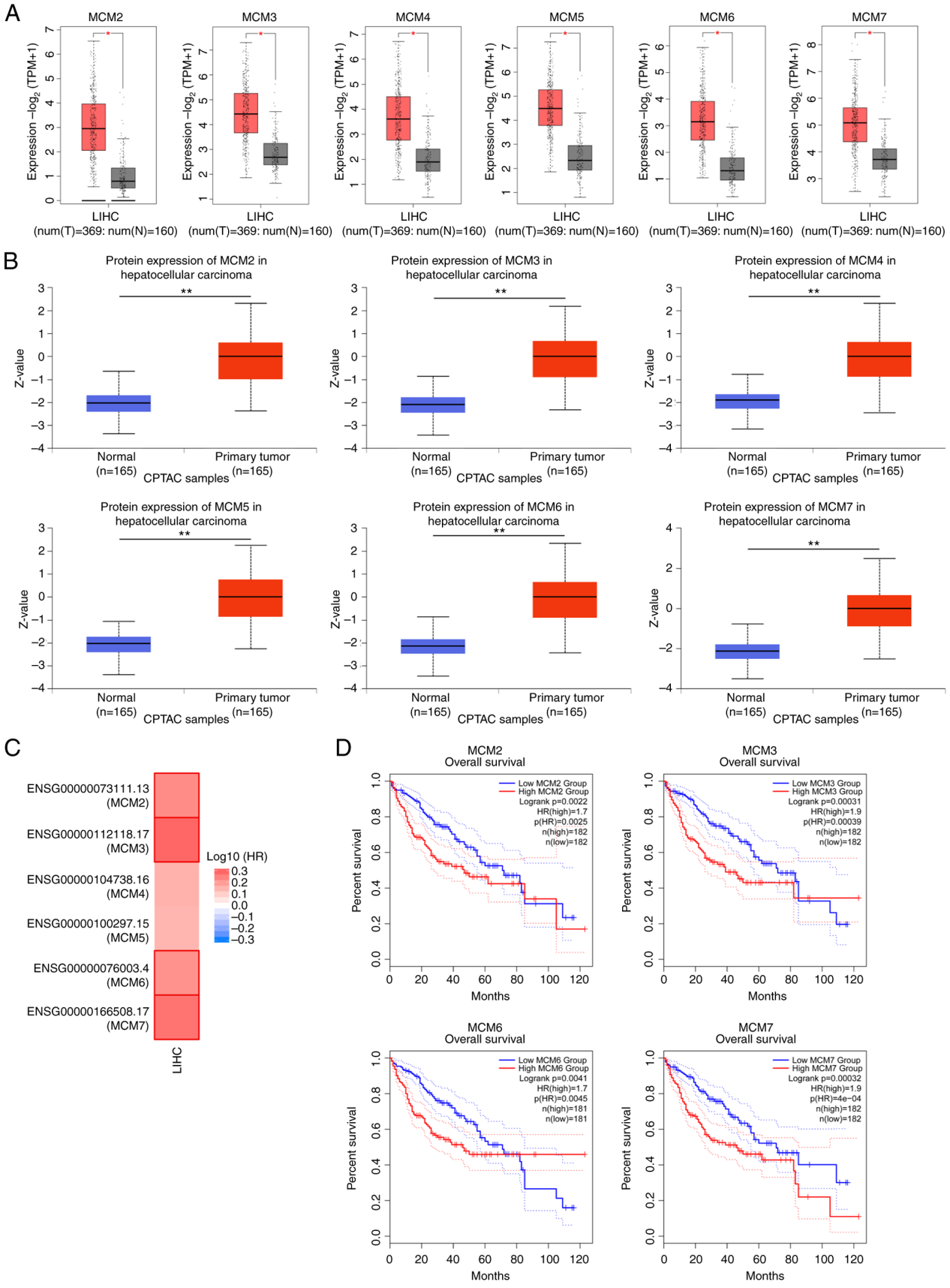

Figure 1. Expression levels and prognostic values of MCM2-7 in human LIHC. (A) mRNA expression levels of MCM2-7 in human LIHC and corresponding normal tissues were analyzed using the GEPIA2 database. *P<0.05. (B) Protein expression levels of MCM2-7 in human hepatocellular carcinoma and corresponding normal tissues were analyzed using the UALCAN database. Z-values represent standard deviations from the median. Log_2 spectral count ratio values from CPTAC were first normalized within each sample profile, and then normalized across samples. **P<0.01. (C) Association of overall survival with MCM2/3/6/7 in LIHC analyzed using the GEPIA2 database. (D) Overall survival rates in patients with LIHC according to the expression levels of MCMs were analyzed using the GEPIA2 database. MCM, minichromosome maintenance protein; LIHC, liver hepatocellular carcinoma; CPTAC, Clinical Proteomic Tumor Analysis Consortium; HR, hazard ratio; p(HR), P-value for the HR; TPM, transcript per million.

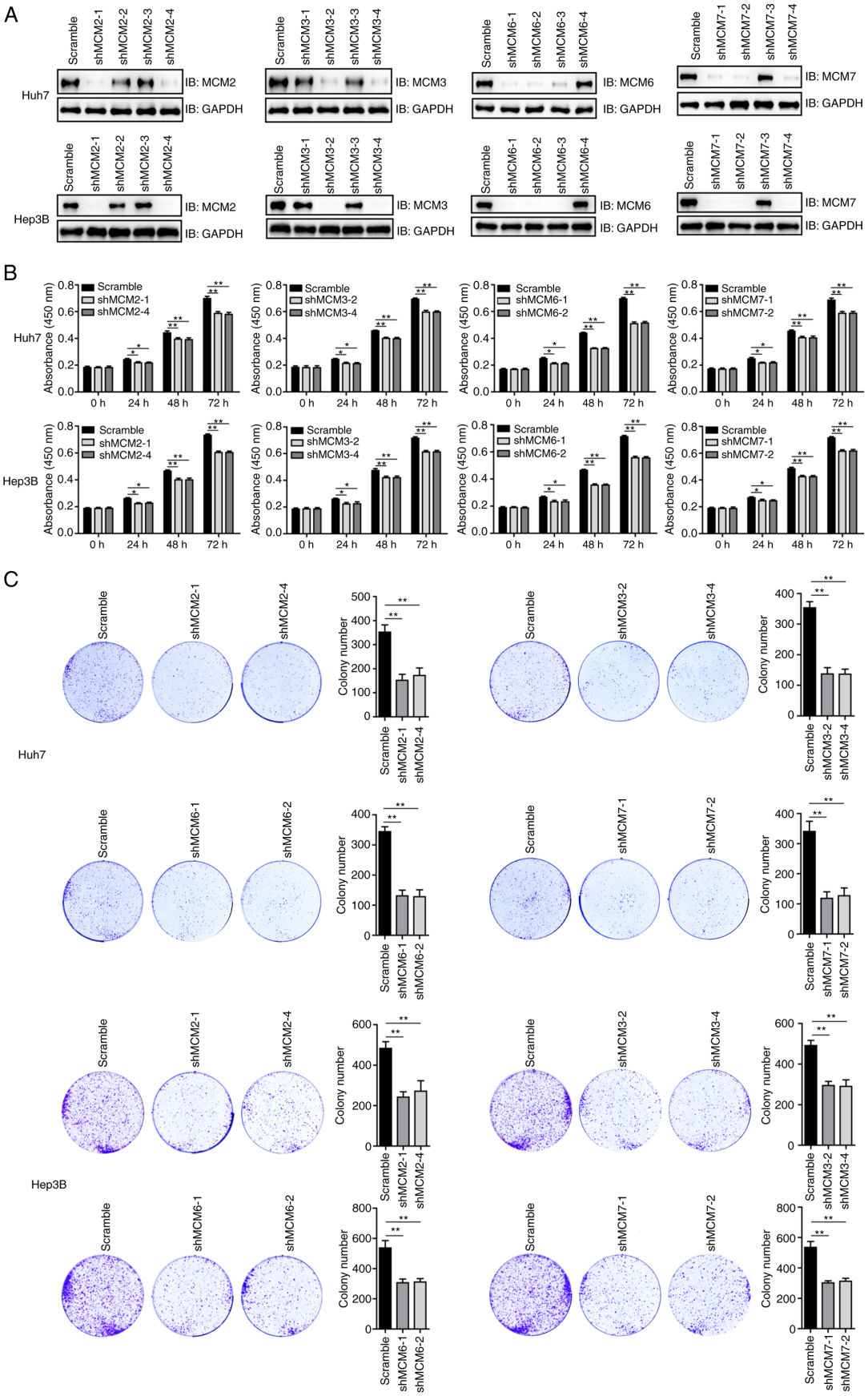

Figure 2. Knockdown of MCMs inhibits the proliferation of HCC cells. (A) Knockdown efficiency of shRNAs targeting MCM2, MCM3, MCM6 and MCM7 as revealed by the IB analysis of Huh7 and Hep3B HCC cells. (B) Knockdown of MCM2, MCM3, MCM6 or MCM7 inhibited the proliferation of HCC cells, as revealed by the cell viability detected using a Cell Counting Kit-8 assay at different time points. The 0 h time point was defined as 6 h after cell seeding. This experiment was repeated three times with six replicates. *P<0.05, **P<0.01. (C) Knockdown of MCM2, MCM3, MCM6 or MCM7 inhibited the colony formation of HCC cells. Three samples were tested per group. **P<0.01. MCM, minichromosome maintenance protein; HCC, hepatocellular carcinoma; sh, short hairpin; IB, immunoblotting; scramble, negative control shRNA.

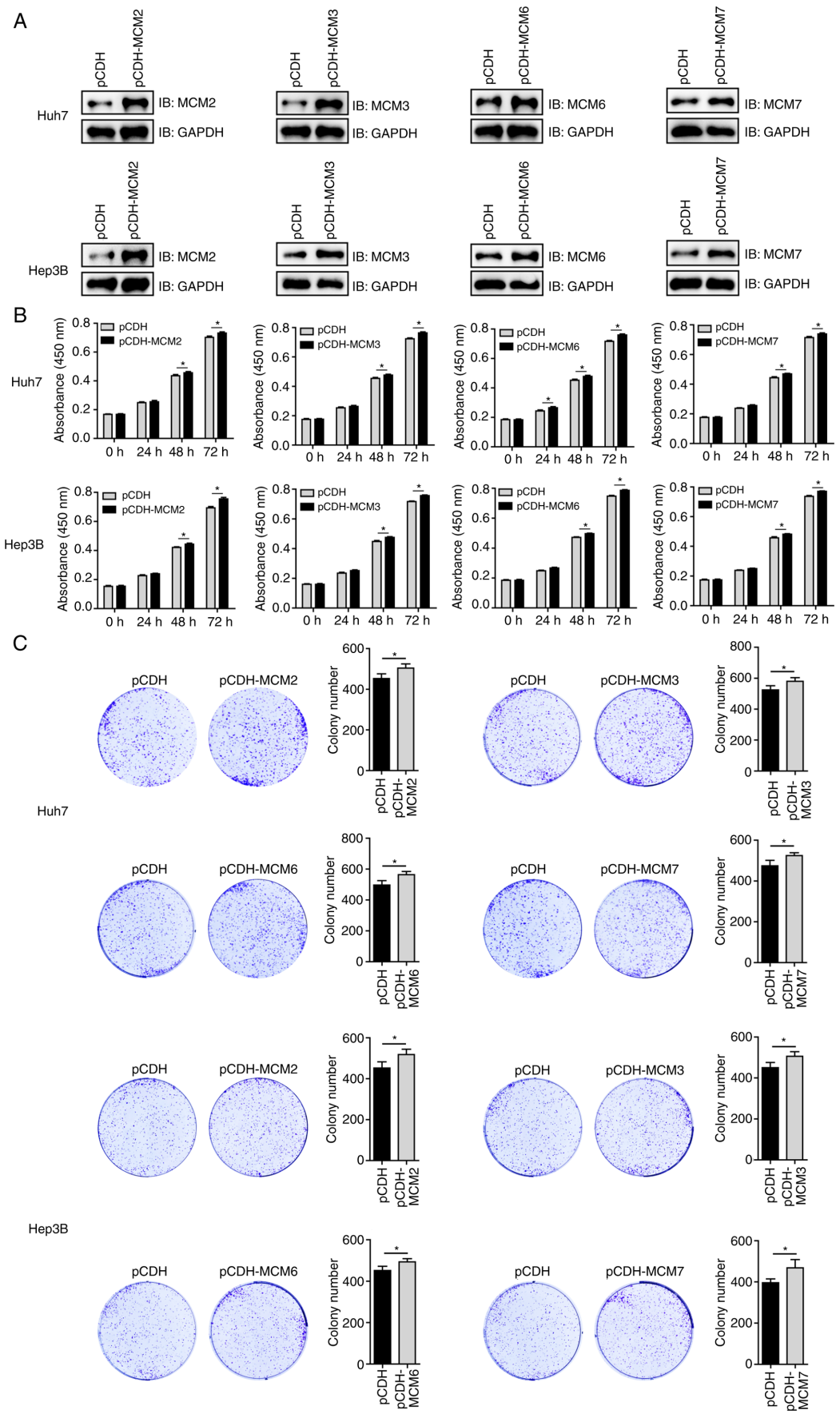

Figure 3. MCMs promote the proliferation of HCC cells. (A) Overexpression efficiency of MCM2, MCM3, MCM6 and MCM7 vectors in Huh7 and Hep3B cells as determined by IB. (B) Overexpression of MCM2, MCM3, MCM6 or MCM7 promoted the proliferation of Huh7 and Hep3B cells as revealed by the cell viability detected using a Cell Counting Kit-8 assay at different time points. The 0 h time point was defined as 6 h after cell seeding. This experiment was repeated three times with six replicates. *P<0.05. (C) Overexpression of MCM2, MCM3, MCM6 or MCM7 promoted the colony formation of HCC cells. Three samples were tested per group. *P<0.05. MCM, minichromosome maintenance protein; HCC, hepatocellular carcinoma; IB, immunoblotting.

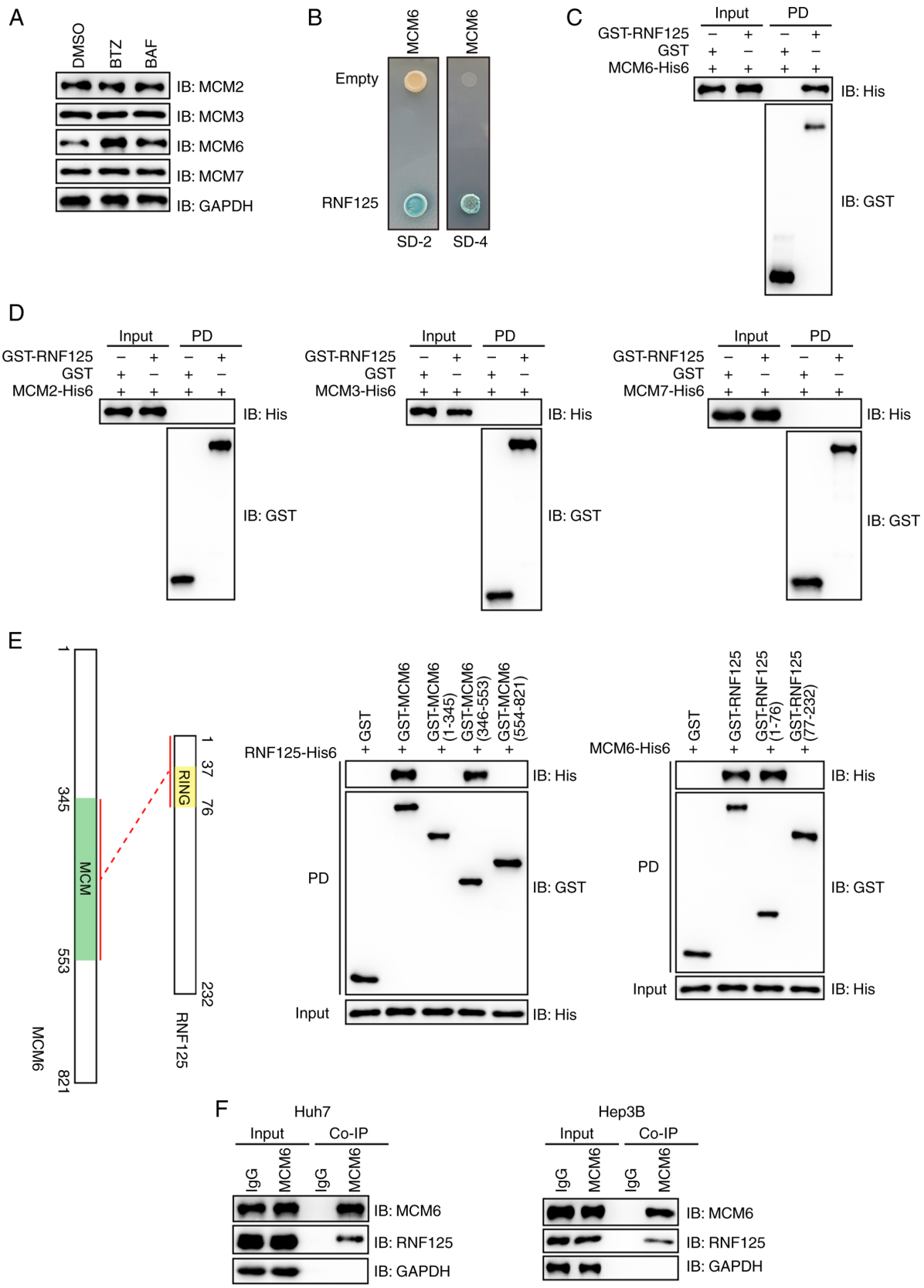

Figure 4. RNF125 interacts with MCM6. (A) Treatment of Huh7 cells with proteasome inhibitor BTZ (1 μmol/l) or autophagy inhibitor BAF (20 nmol/) for 6 h prior to IB analysis indicates that endogenously expressed MCM6 primarily undergoes proteasome-dependent degradation. (B) RNF125 is shown to be an interacting partner for MCM6 using the yeast two-hybrid method, where SD-2 is deficient in leucine and tryptophan, and SD-4 is deficient in uracil, histidine, leucine and tryptophan. (C) Direct interaction between RNF125 and MCM6 was detected by GST PD assay using recombinant GST-RNF125 and MCM6-His6; the GST PD assay was evaluated using IB analysis. (D) No interaction of RNF125 with MCM2, MCM3, and MCM7 was detected by GST pull-down assay with IB analysis. (E) The N-terminal region (1-76 amino acids) containing the RING domain of RNF125 directly interacted with the MCM domain of MCM6. (F) GST PD assays and IB analysis showed that endogenously expressed MCM6 forms a complex with RNF125. The lysates of Huh7 and Hep3B cells were immunoprecipitated with IgG or anti-MCM6 antibody and subjected to IB analysis. RNF125, ring finger protein 125; MCM, minichromosome maintenance; BTZ, bortezomib; BAF, bafilomycin; IB, immunoblotting; GST, glutathione S-transferase; PD, pull-down; Co-IP, co-immunoprecipitation.

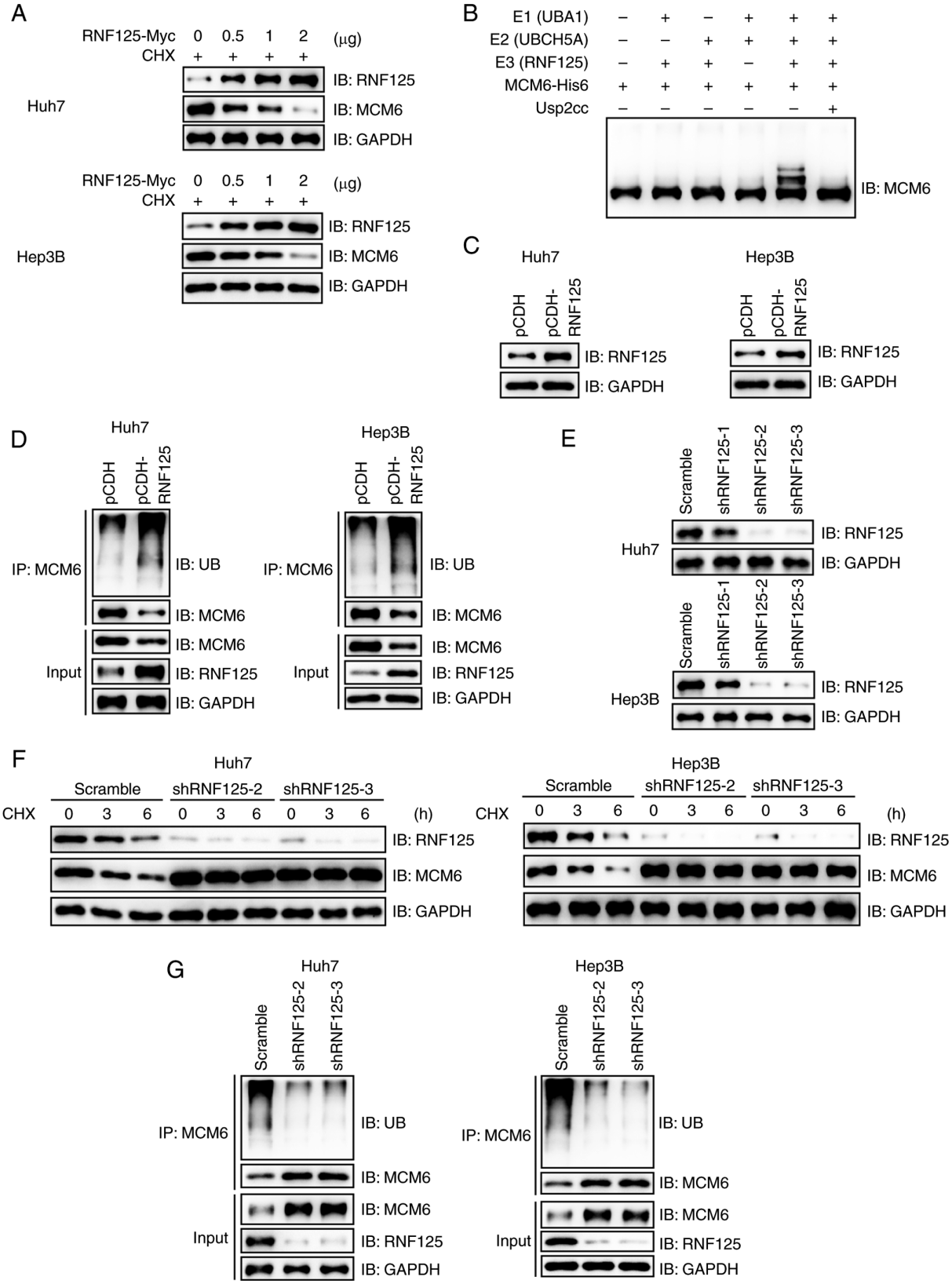

Figure 5. RNF125 promotes the ubiquitination and degradation of MCM6. (A) RNF125 promotes the degradation of MCM6 in a dose-dependent manner, as revealed in Huh7 and Hep3B cells transiently transfected with different amounts of pCDNA3.0-RNF125-Myc or empty vectors and subjected to IB analysis. (B) An *in vitro* ubiquitination assay was performed, and the ubiquitination of MCM6 using different ubiquitination enzymes was detected by IB analysis. The results indicates that RNF125 mediates the ubiquitination of MCM6 *in vitro*. (C) Detection of the protein levels of RNF125 in the lysates of Huh7 and Hep3B cells stably expressing pCDH or pCDH-RNF125. (D) RNF125 promotes the ubiquitination of endogenous MCM6, as revealed by immunoprecipitation of the transfected cells with anti-MCM6 antibody followed by IB analysis. (E) Knockdown efficiency of shRNAs targeting RNF125 in Huh7 and Hep3B cells detected by IB analysis. (F) RNF125 knockdown stabilizes MCM6 in Huh7 and Hep3B cells treated with CHX for different time periods prior to IB analysis. (G) RNF125 knockdown reduces the ubiquitination of endogenous MCM6, as demonstrated by the IP of Huh7 and Hep3B cells stably expressing RNF125 shRNAs with anti-MCM6 antibody prior to IB analysis. RNF125, ring finger protein 125; MCM, minichromosome maintenance protein; IB, immunoblotting; sh, short hairpin; CHX, cycloheximide; IP, immunoprecipitation; Usp2cc, catalytic core of human ubiquitin specific peptidase 2; scramble, negative control.

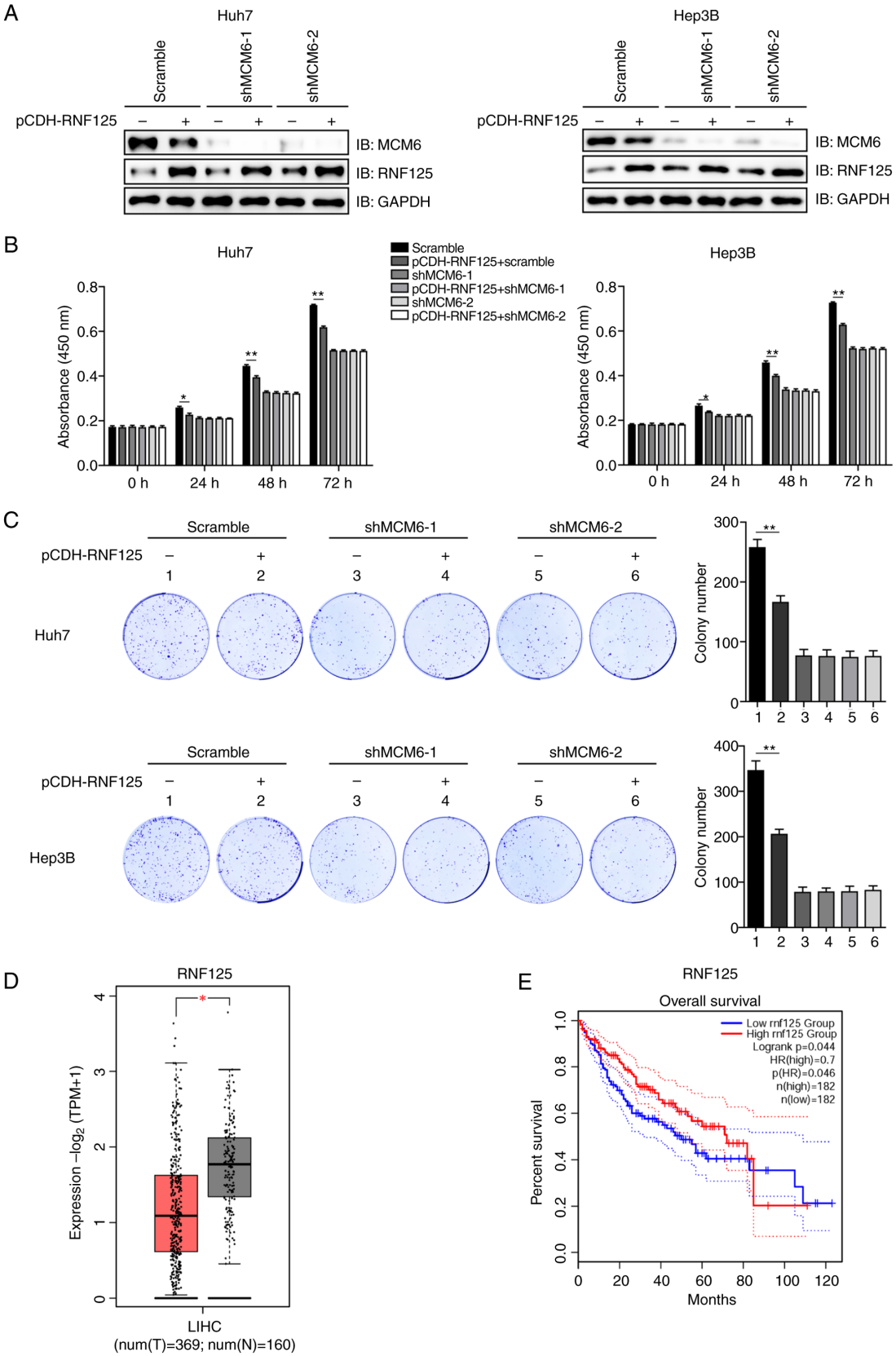

Figure 6. RNF125 promotes the proliferation of HCC cells mainly though MCM6. (A) Detection of the protein expression levels of RNF125 and MCM6 in Huh7 and Hep3B cells stably expressing scramble or MCM6 shRNAs with or without transfection with plasmids containing RNF125 using IB analysis. (B) RNF125 promotes the proliferation of HCC cells via MCM6. The viability of Huh7 and Hep3B cells co-transfected with plasmids expressing RNF125 and shRNAs targeting MCM6 was detected by Cell Counting Kit-8 assay. The experiment was repeated three times with six replicates. *P<0.05, **P<0.01. (C) RNF125 promotes the colony formation of HCC cells though MCM6 in Huh7 and Hep3B cells. Three samples were tested per group. **P<0.01. (D) RNF125 mRNA expression in human LIHC and corresponding normal tissues as analyzed using the GEPIA2 database. *P<0.05. (E) Overall survival rates in patients with LIHC according to the expression level of RNF125 were analyzed using the GEPIA2 database. RNF125, ring finger protein 125; HCC, hepatocellular carcinoma; MCM, minichromosome maintenance protein; scramble, negative control; sh, short hairpin; IB, immunoblotting; HR, hazard ratio; p(HR), P-value for the HR; TPM, transcript per million.

the results showed that patients with LIHC and high mRNA expression of RNF125 had a higher overall survival rate (Fig. 6E). These findings suggest that RNF125 is a potential therapeutic target for human HCC.

Discussion

In the present study, the expression levels and prognostic values of MCM2-7 in human HCC were first analyzed using a public database, and the results suggested that MCM2, MCM3, MCM6 and MCM7 may serve as prognostic markers. The proliferation of human HCC cells was hindered by the knockdown of any of the four MCMs, while the promotion of HCC cell proliferation through the overexpression of these MCMs was shown to have limited effect. It is hypothesized that this may be due to the fact that the MCM complexes function as a complete unit (9); thus, increasing only one type has minimal effects. The homeostasis of these four MCMs was then investigated using a proteasomal or autophagy inhibitor, and the results indicated that only MCM6 was degraded by the proteasome pathway. In addition, RNF125 was identified as an E3 ligase for MCM6, which promoted its ubiquitination and degradation. Further experiments showed that RNF125 promoted the proliferation of HCC cells mainly through MCM6.

The ubiquitin-proteasome pathway is a highly selective protein degradation pathway, which efficiently degrades intracellular proteins and plays an important role in cell proliferation, metabolism and differentiation (24,25). Dysfunction of ubiquitination has been indicated to lead to numerous issues, including cancers and neurodegenerative diseases (22,26,27). RNF125 is a RING-type E3 ubiquitin ligase that features an N-terminal RING domain. Various substrates for RNF125 have been reported, including programmed death-ligand 1 and tripartite motif containing 14 (28,29). The present study has identified MCM6 as a novel substrate for RNF125. Furthermore, it has established that RNF125 primarily impedes the proliferation of HCC cells through MCM6. In addition, analysis using publicly available databases revealed that the expression of RNF125 was lower in LIHC compared with corresponding normal tissues. Moreover, a higher expression level of RNF125 was found to be associated with improved overall survival in patients with LIHC. These findings are consistent with those reported in a previous study (30).

To the best of our knowledge, RNF125 is the first E3 ligase identified for MCM6. Various studies have shown that MCM6 can interact with the E3 ligase UBE3A/E6AP (31,32). However, UBE3A/E6AP is incapable of mediating the ubiquitination of MCM6 (32). Notably, the present study demonstrated that RNF125 does not interact with other MCM family members such as MCM3, MCM2 and MCM7. With the exception of MCM7 (33), no E3 ligases have been reported for other MCM family proteins. The knockdown of MCM2, MCM3 or MCM7 also inhibited the proliferation of HCC cells, indicating that the balance of these proteins is also critical.

The present research has certain limitations. Firstly, the mechanism by which RNF126-MCM6 ubiquitin signaling controls the growth of HCC cells was not examined. Secondly, the findings were not validated in animal models and clinical specimens. Furthermore, the survival analyses were performed using GEPIA2 with the log-rank test the only option for analysis; therefore, it was not possible to exclude the late-stage crossover from the analysis, which may affect the results of the analysis. Therefore, endeavors to test the functions of RNF125-MCM6 axis in animal models and patient samples of LIHC are ongoing. In conclusion, RNF125 and MCM6 are two promising targets for the treatment of LIHC.

Acknowledgements

Not applicable.

Funding

The study was financially supported by the Department of Education of Anhui Province (grant no. 2022AH050774) and the Foundation of Lu'an People's Hospital (grant no. 2022kykt30).

Availability of data and materials

The data generated in the present study may be requested from the corresponding author.

Authors' contributions

XF, DS, XL, YL and PJ performed experiments and data analysis. XF, SW and FL designed and supervised the study. XF and FL wrote the manuscript and provided financial support. XF and FL confirm the authenticity of all the raw data. All authors read and approved the final version of the manuscript.

Ethics approval and consent to participate

Not applicable.

Patient consent for publication

Not applicable.

Competing interests

The authors declare that they have no competing interests.

References

1. Siegel RL, Miller KD, Wagle NS and Jemal A: Cancer statistics, 2023. CA Cancer J Clin 73: 17-48, 2023.
2. Cho SH, You GR, Park C, Cho SG, Lee JE, Choi SK, Cho SB and Yoon JH: Acute respiratory distress syndrome and severe pneumonitis after atezolizumab plus bevacizumab for hepatocellular carcinoma treatment: A case report. World J Gastrointest Oncol 15: 892-901, 2023.
3. Ferrante ND, Pillai A and Singal AG: Update on the diagnosis and treatment of hepatocellular carcinoma. Gastroenterol Hepatol (NY) 16: 506-516, 2020.
4. Le DC, Nguyen TM, Nguyen DH, Nguyen DT and Nguyen LTM: Survival outcome and prognostic factors among patients with hepatocellular carcinoma: A hospital-based study. Clin Med Insights Oncol 17: 11795549231178171, 2023.

5. Marin JJG, Macias RIR, Monte MJ, Romero MR, Asensio M, Sanchez-Martin A, Cives-Losada C, Temprano AG, Espinosa-Escudero R, Reviejo M, *et al*: Molecular bases of drug resistance in hepatocellular carcinoma. Cancers (Basel) 12: 1663, 2020.
6. Saito A, Toyoda H, Kobayashi M, Koiwa Y, Fujii H, Fujita K, Maeda A, Kaneoka Y, Hazama S, Nagano H, *et al*: Prediction of early recurrence of hepatocellular carcinoma after resection using digital pathology images assessed by machine learning. Mod Pathol 34: 417-425, 2021.
7. Wang Y, Chen H, Zhang J, Cheng ASL, Yu J, To KF and Kang W: MCM family in gastrointestinal cancer and other malignancies: From functional characterization to clinical implication. Biochim Biophys Acta Rev Cancer 1874: 188415, 2020.
8. Zhou J, Wang M, Zhou Z, Wang W, Duan J and Wu G: Expression and prognostic value of MCM family genes in osteosarcoma. Front Mol Biosci 8: 668402, 2021.
9. Tye BK: MCM proteins in DNA replication. Annu Rev Biochem 68: 649-686, 1999.
10. Cai HQ, Cheng ZJ, Zhang HP, Wang PF, Zhang Y, Hao JJ, Wang MR and Wan JH: Overexpression of MCM6 predicts poor survival in patients with glioma. Hum Pathol 78: 182-187, 2018.
11. Marnerides A, Vassilakopoulos TP, Boltetsou E, Levidou G, Angelopoulou MK, Thymara I, Kyrtsonis MC, Pappi V, Tsopra O, Panayiotidis P, *et al*: Immunohistochemical expression and prognostic significance of CCND3, MCM2 and MCM7 in Hodgkin lymhoma. Anticancer Res 31: 3585-3594, 2011.
12. Wojnar A, Pula B, Piotrowska A, Jethon A, Kujawa K, Kobierzycki C, Rys J, Podhorska-Okolow M and Dziegiel P: Correlation of intensity of MT-I/II expression with Ki-67 and MCM-2 proteins in invasive ductal breast carcinoma. Anticancer Res 31: 3027-3033, 2011.
13. Wu W, Wang X, Shan C, Li Y and Li F: Minichromosome maintenance protein 2 correlates with the malignant status and regulates proliferation and cell cycle in lung squamous cell carcinoma. Onco Targets Ther 11: 5025-5034, 2018.
14. Stewart PA, Khamis ZI, Zhau HE, Duan P, Li Q, Chung LWK and Sang QA: Upregulation of minichromosome maintenance complex component 3 during epithelial-to-mesenchymal transition in human prostate cancer. Oncotarget 8: 39209-39217, 2017.
15. Liu M, Hu Q, Tu M, Wang X, Yang Z, Yang G and Luo R: MCM6 promotes metastasis of hepatocellular carcinoma via MEK/ERK pathway and serves as a novel serum biomarker for early recurrence. J Exp Clin Cancer Res 37: 10, 2018.
16. Vigouroux C, Casse JM, Battaglia-Hsu SF, Brochin L, Luc A, Paris C, Lacomme S, Gueant JL, Vignaud JM and Gauchotte G: Methyl(R217)HuR and MCM6 are inversely correlated and are prognostic markers in non small cell lung carcinoma. Lung Cancer 89: 189-196, 2015.
17. Zheng T, Chen M, Han S, Zhang L, Bai Y, Fang X, Ding SZ and Yang Y: Plasma minichromosome maintenance complex component 6 is a novel biomarker for hepatocellular carcinoma patients. Hepatol Res 44: 1347-1356, 2014.
18. Tang Z, Li C, Kang B, Gao G, Li C and Zhang Z: GEPIA: A web server for cancer and normal gene expression profiling and interactive analyses. Nucleic Acids Res 45: W98-W102, 2017.
19. Chandrashekar DS, Bashel B, Balasubramanya SAH, Creighton CJ, Ponce-Rodriguez I, Chakravarthi BVSK and Varambally S: UALCAN: A portal for facilitating tumor subgroup gene expression and survival analyses. Neoplasia 19: 649-658, 2017.
20. Li C, Lu W, Yang L, Li Z, Zhou X, Guo R, Wang J, Wu Z, Dong Z, Ning G, *et al*: MKRN3 regulates the epigenetic switch of mammalian puberty via ubiquitination of MBD3. Natl Sci Rev 7: 671-685, 2020.
21. Wang CC, Peng H, Wang Z, Yang J, Hu RG, Li CY and Geng WJ: TRIM72-mediated degradation of the short form of p62/SQSTM1 rheostatically controls selective autophagy in human cells. Mil Med Res 9: 35, 2022.
22. Yang Y, Luo Y, Yang C, Hu R, Qin X and Li C: TRIM25-mediated ubiquitination of G3BP1 regulates the proliferation and migration of human neuroblastoma cells. Biochim Biophys Acta Gene Regul Mech 1866: 194954, 2023.
23. Li C, Han T, Li Q, Zhang M, Guo R, Yang Y, Lu W, Li Z, Peng C, Wu P, *et al*: MKRN3-mediated ubiquitination of Poly(A)-binding proteins modulates the stability and translation of GNRH1 mRNA in mammalian puberty. Nucleic Acids Res 49: 3796-3813, 2021.
24. Mansour MA: Ubiquitination: Friend and foe in cancer. Int J Biochem Cell Biol 101: 80-93, 2018.
25. Sheng X, Xia Z, Yang H and Hu R: The ubiquitin codes in cellular stress responses. Protein Cell: pwad045, 2023 (Epub ahead of print).
26. Liu Z, Chen P, Gao H, Gu Y, Yang J, Peng H, Xu X, Wang H, Yang M, Liu X, *et al*: Ubiquitylation of autophagy receptor Optineurin by HACE1 activates selective autophagy for tumor suppression. Cancer Cell 26: 106-120, 2014.
27. Xu X, Li C, Gao X, Xia K, Guo H, Li Y, Hao Z, Zhang L, Gao D, Xu C, *et al*: Excessive UBE3A dosage impairs retinoic acid signaling and synaptic plasticity in autism spectrum disorders. Cell Res 28: 48-68, 2018.
28. Jiang C, He L, Xiao S, Wu W, Zhao Q and Liu F: E3 ubiquitin ligase RNF125 suppresses immune escape in head and neck squamous cell carcinoma by regulating PD-L1 expression. Mol Biotechnol 65: 891-903, 2023.
29. Jia X, Zhou H, Wu C, Wu Q, Ma S, Wei C, Cao Y, Song J, Zhong H, Zhou Z and Wang J: The ubiquitin ligase RNF125 targets innate immune adaptor protein TRIM14 for ubiquitination and degradation. J Immunol 198: 4652-4658, 2017.
30. Feng Z, Ke S, Wang C, Lu S, Xu Y, Yu H, Li Z, Yin B, Li X, Hua Y, *et al*: RNF125 attenuates hepatocellular carcinoma progression by downregulating SRSF1-ERK pathway. Oncogene 42: 2017-2030, 2023.
31. Martínez-Noël G, Luck K, Kühnle S, Desbuleux A, Szajner P, Galligan JT, Rodriguez D, Zheng L, Boyland K, Leclere F, *et al*: Network analysis of UBE3A/E6AP-associated proteins provides connections to several distinct cellular processes. J Mol Biol 430: 1024-1050, 2018.
32. Li C, Han T, Guo R, Chen P, Peng C, Prag G and Hu R: An integrative synthetic biology approach to interrogating cellular ubiquitin and ufm signaling. Int J Mol Sci 21: 4231, 2020.
33. Kühne C and Banks L: E3-ubiquitin ligase/E6-AP links multicopy maintenance protein 7 to the ubiquitination pathway by a novel motif, the L2G box. J Biol Chem 273: 34302-34309, 1998.